The Effect of Apical and Basolateral Lipids on the Function of the Band 3 Anion Exchange Protein

Wouter van't Hof,* Abha Malik,‡ S. Vijayakumar,‡ Jizeng Qiao,‡ Janet van Adelsberg,‡ and Qais Al-Awqati‡

*Department of Cell Biology and Anatomy, Cornell Medical College, New York 10021; and ‡Departments of Medicine and Physiology, College of Physicians and Surgeons of Columbia University, New York 10032

Abstract. Although many polarized proteins are sorted to the same membrane domain in all epithelial tissues, there are some that exhibit a cell type–specific polarity. We recently found that band 3 (the anion exchanger AE1) was present in the apical membrane of a renal intercalated cell line when these cells were seeded at low density, but its targeting was reversed to the basolateral membrane under the influence of an extracellular matrix protein secreted when the cells were seeded at high density. Because apical and basolateral lipids differ in epithelia, we asked what effect might these lipids have on band 3 function. This question is especially interesting since apical anion exchange in these cells is resistant to disulfonic stilbene inhibitors while basolateral anion exchange is quite sensitive. Furthermore, the apical anion exchanger cannot be stained by antibodies that readily identify the basolateral protein.

We used short chain sphingolipid analogues and found that sphingomyelin was preferentially targeted to the basolateral domain in the intercalated cell line. The ganglioside GM_1 (Gal $1\beta1$, 3GalNAc$\beta1$, 4Gal-NeuAc$\alpha2$, 3Gal$\beta1$, 4Glc ceramide) was confined to the apical membrane as visualized by confocal microscopy after addition of fluorescent cholera toxin to filter grown cells. We reconstituted erythrocyte band 3 into liposomes using apical and basolateral types of lipids and examined the inhibitory potency of 4,4′-dinitorsostilbene-2,2′-disulfonic acid (DNDS; a reversible stilbene) on $^{35}SO_4/SO_4$ exchange. Although anion exchange in sphingomyelin liposomes was sensitive to inhibition, the addition of increasing amounts of the ganglioside GM_1 reduced the potency of the inhibitor drastically. Because these polarized lipids are present in the exofacial surface of the bilayer, we propose that the lipid structure might influence the packing of the transmembrane domains of band 3 in that region, altering the binding of the stilbenes to these chains. These results highlight the role of polarized lipids in changing the function of unpolarized proteins or of proteins whose locations differ in different epithelia.

Tₕₑ plasma membrane of epithelia is differentiated into two domains that have different lipid and protein composition. The apical membrane is highly enriched in glycosphingolipids, while the basolateral membrane contains higher concentration of phosphatidyl choline and sphingomyelin (Simons and van Meer, 1988). While an individual polarized protein is usually targeted to the same domain in all types of epithelial cells, some exhibit a cell type–specific polarity. For instance, the α subunit of the Na,K ATPase is present in the basolateral membrane of most epithelia but is targeted to the apical membrane of the retinal pigment epithelium and choroid plexus (Gundersen et al., 1993). The human LDL receptor transgene is expressed as an apical protein in mouse kidneys but as a basolateral protein in their intestine (Pathak et al., 1990). GPI-linked proteins are targeted to the apical membrane of most epithelia (Lisanti and Rodriguez-Boulan, 1990) but go to the basolateral membrane of a thyroid cell line (Zurzolo et al., 1993). We recently discovered that the renal anion exchanger, band 3 (AE1), is targeted to the apical membrane of an immortalized intercalated cell line, but the protein could be retargeted to the basolateral membrane in the same cell line if the cells were seeded at high density (van Adelsberg et al., 1994). Given that transport proteins and receptors are embedded in the lipid bilayer, we asked whether the function of an individual protein such as band 3 could be altered by the radically different lipids in these two membrane domains.

The intercalated epithelial cells of the renal collecting tubule are specialized for transepithelial H^+ or HCO_3^- transport and exist in a variety of types, with two forms, α

Address all correspondence to Qais Al-Awqati, Department of Medicine, College of Physicians and Surgeons of Columbia University, 630 W. 168th St., New York, NY 10032. Tel.: (212) 305-3512. Fax: (212) 305-3475. E-mail: qa1@columbia.edu

and β, probably representing the extreme ends of a spectrum (for review see Schuster, 1993; Al-Awqati, 1996). The "canonical" α cell has an apical H^+ ATPase and a basolateral Cl/HCO_3 exchanger, which is a form of the red cell band 3 (Drenckhahn et al., 1985; Brown et al., 1988). In the β type, HCO_3^- is secreted by an apical Cl/HCO_3 exchanger and a basolateral H^+ ATPase. In earlier studies, we found that when rabbits were fed an acid diet, the number of α cells increased while the number of β cells decreased, but the total number of intercalated cells remained the same. We concluded that β cells converted to α cells and termed this process plasticity in epithelial polarity (Schwartz et al., 1985). The question then arose whether the apical Cl/HCO_3 exchanger is the same as the basolateral protein. Molecular cloning showed that the kidney anion exchanger is an alternately spliced form of AE1 missing the first three exons (Brosius et al., 1989; Kudrycki and Shull, 1989). The same antibodies that readily stained the basolateral anion exchanger have consistently failed to stain the apical membranes of β cells. In addition, while basolateral Cl/HCO_3 exchange is sensitive to inhibition by 4,4′-diisothiocyanostilbene-2,2-disulfonic acid (DIDS),[1] apical exchange is not (Schuster, 1985; Kohn et al., 1990). These studies suggested that the two polarized Cl/HCO_3 exchangers might be different proteins.

To test some of these ideas directly, we recently generated a clonal β intercalated cell line that exhibited all their previously known characteristics: apical Cl/HCO_3 exchange, basolateral H^+ ATPase, an apical peanut lectin binding protein, a basolateral glucose transporter, and no apical endocytosis (Edwards et al., 1992). Staining with an anti–band 3 antibody that was affinity purified against the cytoplasmic domain of erythrocyte AE1 showed that these cells, like their in vivo counterparts, had no apical staining. Surprisingly however, we found that these antibodies were able to identify this protein in isolated apical membranes by immunoblot analysis (van Adelsberg et al., 1993). The cells also expressed the mRNA for AE1. More interestingly, we found that when these cells were plated at subconfluent density and analyzed after they became polarized monolayers, they had AE1 in their isolated apical membranes. However, when seeded at high density, these cells exhibited all the characteristics of α cells; basolateral AE1, vigorous apical endocytosis, and apical H^+ ATPase (van Adelsberg et al., 1994). They continued to express GLUT1 (the glucose transporter) in the basolateral membrane and peanut lectin binding protein in the apical membrane. A large protein (which we termed hensin) was deposited by these cells into their extracellular matrix, and when purified, it was able to reverse the polarity of band 3 even in the low density cells (van Adelsberg et al., 1994; Takito et al., 1996). Because this is a clonal cell line, these in vitro studies demonstrate that conversion of β cells to α cells is feasible, at least in principle. But whether this density-dependent change in phenotype is similar to what occurs in vivo will require more studies.

There have been other examples in which the same protein has different characteristics when it is located in different membrane domains. In one clone of Madin-Darby canine kidney cells (MDCK), 50% of newly synthesized Na,K ATPase is targeted to the apical membrane, where its sensitivity to ouabain (Hammerton et al., 1991) or biotinylation reagents (Gottardi et al., 1995) was found to be reduced. Furthermore, the apical bradykinin B2 receptor has higher affinity for its ligand than when it is in the basolateral membrane (Denning and Welsh, 1991). What effect could apical or basolateral lipids have on the function of receptors and transporters in these two membrane domains? In particular, could this explain the lack of sensitivity of apical band 3 to its specific inhibitors in the intercalated cells? Indeed, when we tested this hypothesis by reconstitution of erythrocyte band 3 in liposomes whose composition is similar to those of the apical membrane, the anion exchanger became resistant to inhibition by disulfonic stilbenes. These results highlight the influence that lipid polarity might have on the function of proteins that are unpolarized or whose polarity can change from one surface to another.

Materials and Methods

C_6-NBD Sphingolipid Transport Assay

Intercalated cells were maintained as described previously (Edwards et al., 1992; van Adelsberg et al., 1994). For lipid polarity experiments, cells were plated on 0.4-μm pore size, 4.7-cm^2 Transwells (Costar, Cambridge, MA) at low density (2×10^4 cells/cm^2) or at high density (5×10^5 cells/cm^2) and grown for 9–12 d at 39°C. Delivery of C_6-NBD-sphingolipids to the cell surface was assayed as before (van't Hof and van Meer, 1990, 1994). Incorporation of lipids into cells or extraction from cells was performed by the addition of lipid-loaded BSA or lipid-free BSA, respectively, to the medium for a specific amount of time. The transfer of lipids from the cell membrane to the reservoir of delipidated BSA is termed "back-exchange" (Pagano and Martin, 1988). In brief, the fluorescent precursor, C_6-NBD-ceramide (N-6[7-nitro-2,1,3,-benzoxadiazol-4-yl] aminocaproyl-sphingosine) was incorporated into filter-grown cells for 30 min at 10°C by exchange from BSA-NBD-lipid complexes (van Helvoort et al., 1966; van Meer et al., 1987). 1 ml of NBD-ceramide (10 μM) in HBSS containing 0.03% BSA (wt/vol) was added to the apical surface of the monolayer. Transport of intracellularly synthesized C_6-NBD-glucosyl ceramide (C_6-NBD-Glc/Cer) and C_6-NBD-sphingomyelin (C_6-NBD-SM) to the cell surface was assayed for 1 h at 37°C by continuous depletion from the cell surface by BSA (1% in HBSS wt/vol) in the apical or basolateral media. This was followed by another back-exchange against HBSS-BSA for 30 min at 10°C to maximize depletion. Fluorescent lipids were extracted from the combined apical media, the combined basal media, and the cell monolayer on the filter, after which they were quantitatively analyzed by HPTLC followed by measurement of NBD-fluorescence in the individual lipid spots (van Meer et al., 1987). The "polarity" of each lipid is defined as the ratio of apical to basolateral delivery. The quotient of these ratios, the "relative polarity" (Glc/Cer to SM ratio), can be used as a measure of differential transport of Glc/Cer from SM (van't Hof and van Meer, 1990). Six independent experiments were performed in high-density cells and another six in low density cells. The results are presented as the means ± SEM.

Reconstitution of Erythrocyte Band 3

Unless otherwise stated, all the steps were carried out at 0–4°C. 100 ml of rabbit blood, aseptically collected in Na citrate, was received from Pel Freeze. It was repeatedly washed with 5 vol of 0.9% NaCl and centrifuged four or five times at 5,000 rpm. The resulting red cell pellet was resuspended in 10 vol of Na phosphate buffer (5 mM NaPO₄, 0.2 mM DTT, 20 μg/ml PMSF, pH 8.0) and incubated on ice for 10 min. The suspension was then centrifuged at 15,000 rpm for 20 min in a rotor (model SA600; Dupont Instruments, Newtown, CT). The pellet was subjected to seven or

---

1. *Abbreviations used in this paper*: Cer, ceramide; DIDS, 4,4′- diisothiocyanostilbene-2,2-disulfonic acid; DNDS, 4,4′-dinitorsostilbene-2,2′-disulfonic acid; Glc/Cer, glucosylceramide; GM_1, ganglioside GM_1 (Gal 1β1, 3GalNAcβ1, 4Gal-NeuAcα2, 3Galβ1, 4Glc ceramide); GSL, glycosphingolipids; SM, sphingomyelin; PC, phosphatidylcholine.

eight similar washings until the supernatant was clear. The washed ghosts were frozen at −70°C. Aliquots of these ghosts were then thawed and washed once again in 10 vol of Na phosphate buffer, pH 8.0, and the pellet was resuspended in hypotonic buffer (2 mM EDTA, 2 mM DTT, 1 mM PMSF, pH 8.0) and centrifuged at 15,000 rpm for 20 min as above. The resulting pellet was resuspended in the hypotonic buffer, pH 8.0 and incubated at 37°C for 30 min, followed by centrifugation at 15,000 rpm or 20 min. This was repeated twice. The pellet was then resuspended in buffer containing 1M KI, 1 mM EDTA, 1 mM DTT, 20 μg/ml PMSF, pH 7.4, and incubated at 37°C for 30 min. The suspension was centrifuged twice at 20,000 rpm for 20 min. The final pellet was suspended in 5 mM Na phosphate buffer, pH 7.4, and stored at −70°C. This method is that published previously by Casey et al. (1989).

To reconstitute band 3 into purified lipids, we added a 25-fold excess of the lipid (wt/wt) to stripped red cell ghosts followed by cycles of freeze–thaw and sonication (Sekler et al., 1995). Lipids were obtained from Avanti Polar Lipids (Alabaster, AL) (sphingomyelin or phosphatidyl choline) or from Matreya, Inc. (Pleasant Gap, PA) (monosialoganglioside [GM$_1$] or ceramide). The lipids (usually dissolved in chloroform) were first dried under argon and resuspended in sulfate buffer (2 mM MgSO$_4$, 20 mM Na$_2$SO$_4$, and 10 mM MES, pH 5.5) in a final volume of 125 μl, in the presence or absence of 4,4′-dinitorsostilbene-2,2′-disulfonic acid (DNDS; Pfaltz and Bauer, Inc., Waterbury, CT). After 15 successive 1-s sonication cycles using a bath sonicator (model 2200; Branson Ultrasonic Corp., Danbury, CT), the lipids were then mixed with stripped ghost protein containing 50 μg of stripped red cell ghost protein in a final volume of 150 μl. This reconstitution mixture was subjected to one cycle of rapid freezing in liquid nitrogen and thawing at room temperature, followed by a timed 30-s sonication in the bath sonicator.

$^{35}SO_4/SO_4$ Exchange

For each assay point, 25 μl proteoliposomes (containing 8.3 μg of stripped ghost protein with 25-fold excess of lipids) were incubated at 37°C for 5 min, and sulfate transport was initiated by adding an equal volume of [$^{35}SO_4$] 10 μCi/ml (250–1,000 mCi/mmol; Dupont/NEN, Boston, MA) in sulfate buffer in the presence or absence of DNDS. The proteoliposomes were incubated with radioactive $^{35}SO_4$ at 37°C for 1, 3, 5, 10, and 20 min. Uptake was terminated by passing a 50-μl sample through an anion exchange column (Amberlite IRN-78; Polysciences, Inc., Warrington, PA). The column was first preequilibrated with 80 mM sucrose; the sample was then loaded and chased with 300 μl of the sucrose buffer. The liposomes were then eluted with 600 μl of the sucrose medium and counted. The columns were prepared as described previously (Landry et al., 1987). The resin was first washed several times with dH$_2$O, and the pH of the resin was adjusted to 1.5 with 2 vol of 50% D-gluconic acid (wt/wt) (Sigma Chemical Co., St. Louis, MO). The resin was incubated at room temperature for 2 h and then repeatedly washed with distilled water until the pH reached 3.5. It was then packed into 7-cm glass Pasteur pipettes using minimal amounts of glass wool as a plug.

In each study, the uptake into liposomes containing band 3 was always compared with that in protein-free liposomes, and the results represent the protein-mediated transport rate. In some experiments, red cell ghost protein was initially treated with 1 mM DIDS at 4°C for 1 h, followed by addition of lipids and freeze–thaw sonication cycle as above; these uptake studies represented the fluxes not due to band 3 and were largely similar to the uptake in the absence of protein. All flux studies were performed at 37°C and at pH 5.5. For studies with DNDS, the drug was present in equal concentrations inside and outside the liposomes. In any individual experiment, each time point was the average of triplicate measurements. The fluxes were averaged for each experiment and analyzed statistically when three or more independent experiments had been performed.

Densitometric analysis of Coomassie blue–stained polyacrylamide gels of the stripped ghost proteins showed that band 3 accounted for 60–73% of the stained proteins, but this is likely to be an overestimate (by perhaps twofold) because of the presence of glycophorins and other red cell proteins in this molecular weight range. To estimate the amount of band 3 protein present in the proteoliposomes that were assayed for their $^{35}SO_4$ uptake, we used immunoblots with a previously characterized antibody (van Adelsberg et al., 1993), comparing known amounts of stripped ghost protein with fractions of proteoliposomes before and after passage through the anion exchange resin. The reconstitution method and the assay procedure resulted in losses of band 3 that differed in each lipid used. The recovery in the final assay, as percentage of input band 3, was 79% in phosphatidylcholine (PC), 39% in SM, and 13% in SM + 30% GM$_1$.

These recoveries were used to "correct" the band 3–mediated rate of transport to estimate the turnover number of the reconstituted protein.

We estimated the orientation of band 3 in these proteoliposomes by measuring $^{35}SO_4$ influx into PC and SM + 30% GM$_1$ liposomes in the absence of drugs, or after addition of 1 mM DIDS to the outside. These were compared with uptake into proteoliposomes made with red cell protein that had been pretreated with 1 mM DIDS. In PC liposomes, 70% of the band 3–mediated flux was inhibited by external DIDS, while in SM +30% GM$_1$ liposomes, extravesicular DIDS inhibited the flux by 44%.

Immunocytochemistry

The immortalized intercalated cells were plated at high or low density on Transwell filters with 0.4-μm pores and grown at 40°C for 5 d. Cells were then washed three times with PBS (145 mM NaCl, 4 mM KCl, 10 mM phosphate, pH 7.4), fixed for 5 min in 2% (wt/vol) paraformaldehyde, and quenched with 50 mM NH$_4$Cl in PBS for 15 min. The fixed cell monolayers were incubated (on both the apical and basolateral side) in PBS containing 500 μg/ml rhodamine-conjugated cholera toxin B subunit (List Biological Laboratories, Campbell, CA) for 2 h at 4°C. The monolayers were then washed three times in PBS and incubated for 1 h with 1:50 dilution of mouse anti–collagen type IV IgG (BIODESIGN International, Kennebunkport, ME) in PBS containing 3% BSA at 4°C. After three washes with PBS containing BSA, the monolayers were incubated in 1:100 dilution of FITC-labeled goat anti–mouse antibody (Jackson ImmunoResearch, West Grove, PA) for 1 h. Finally, the cell monolayers were washed in PBS containing BSA as well as PBS and mounted in 90% glycerol in PBS with 0.1% p-phenylenediamine and viewed by an Axiovert 100 laser scanning confocal microscope (model LSM 410; Carl Zeiss, Inc., Jena, Germany). Excitation was accomplished with an argon-krypton laser producing lines at 488 or 568 nm. The images were collected at 1-μm thickness optical sections and analyzed by the Zeiss LSM-PC software. The images were processed with Adobe Photoshop software (San Jose, CA).

Results

Polarized Lipid Distribution in Intercalated Cells

When the exchangeable lipid C$_6$-NBD-ceramide is added to cells via liposomes or BSA complexes, it rapidly penetrates into the cells by exchange through the water phase and translocation across the plasma membrane (Pagano and Martin, 1988). Subsequently, it diffuses through the cytoplasm before it concentrates in the Golgi complex, where it is metabolically converted into C$_6$-NBD-Glc/Cer, a glycolipid analogue, and C$_6$-NBD-SM, a phospholipid analogue (Lipsky and Pagano, 1985). Transport to the plasma membrane of these products can be monitored by "back-exchange," the selective depletion of the exchangeable lipids from the cell surface by excess lipid-free BSA added to the media (Lipsky and Pagano, 1985).

The analysis of the biosynthesis and transport of C$_6$-NBD-Glc/Cer and C$_6$-NBD-SM to the plasma membrane in epithelial cells grown on permeable Transwell supports provides a simple assay to study polarized delivery of lipids to the apical and basolateral cell surface domains (van Meer et al., 1987; van't Hof and van Meer, 1990). Control experiments have shown that C$_6$-NBD-lipids present in one domain cannot be depleted by BSA added to the media in contact with the opposite domain, indicating that the assay measures transport of lipids to the apical and basolateral domain separately (van't Hof and van Meer, 1990). In these studies, it was observed that in MDCK and Caco-2 epithelial cells, C$_6$-NBD-Glc/Cer is targeted to the apical domain, while C$_6$-NBD-SM is preferentially delivered to the basolateral cell surface. As this lipid sorting phenomenon is identical to the lipid polarity observed in epithelial cells in vivo and in vitro (for a recent review see van't Hof and van Meer,

1994), the intracellular sorting of the C6-NBD-sphingolipid analogues reflects that of their endogenous counterparts.

After labeling of filter-grown intercalated epithelial cells with C_6-NBD-ceramide for 30 min at 10°C (to allow for efficient incorporation of the ceramide precursor into the Golgi), transport of newly synthesized C_6-NBD-lipid products was monitored as a function of time at 37°C (Fig. 1) by back-exchange against BSA added to the apical and basolateral media. After 30, 60, and 120 min, newly synthesized C_6-NBD-Glc/Cer was observed to be targeted about equally to both domains, with a slight apical tendency (Fig. 1, *top*; apical/basolateral sorting, 1.0 ± 0.1). Recall, however, that what is being measured is the targeting of glucosylceramide (Glc/Cer), but given that the apical surface is only a fraction of the basolateral surface (the absolute values in these cells will need to be defined), then the concentration of Glc/Cer in the apical membrane is much higher than in the basolateral membrane. C_6-NBD-SM was found to be preferentially targeted to the basolateral domain (Fig. 1, *middle*; apical/basolateral 0.5 ± 0.1). The relative polarity of Glc/Cer to SM ratio (van't Hof and van Meer, 1990) shows a twofold apical enrichment of Glc/Cer over SM (Fig. 1, *bottom*; 2.0 ± 0.2), or, in other words, in a twofold basolateral enrichment of SM over Glc/Cer. Polarized delivery of NBD-lipids was identical in low-density (Fig. 1) and high-density intercalated cells (not shown). In this respect, polarized steady-state distribution of lipids was similar to that of the peanut lectin binding protein, which was apical in both cell types, and the glucose transporter, which was basolateral in both.

A significant fraction of cellular glycolipids consists of gangliosides, which are negatively charged because of the presence of neuraminic (sialic) acids. In epithelial cells, gangliosides such as GM_1 may be found on both surface domains, as judged by the binding of cholera toxin (Lencer et al., 1992). However, when values are expressed as percentages of total ganglioside, individual gangliosides are found to display asymmetric distributions in apical (brush-border) or basolateral membranes from renal kidney epithelial cells (Spiegel et al., 1988). The apical domains are relatively enriched in GM_3, GM_1, and GD_{1a}, while basolateral domains contain higher amounts of GD_3 and GM_4. However, we emphasize that total glycosphingolipids (composed of gangliosides and other glycosphingolipids [GSLs]), constitute as much as 33% of the total apical lipids while forming 7% of the basolateral lipids (Kawai et al., 1974; Spiegel et al., 1988).

The B-subunit of cholera toxin binds specifically to GM_1 (Cuatrecasas, 1973), and we found that rhodamine-labeled cholera toxin binding was localized entirely in the apical domain using confocal fluorescence microscopy (Fig. 2). In these studies, cholera toxin was added to basal and apical media simultaneously with antibodies to collagen IV, which is present in intracellular vesicles and is deposited in the basal ECM in these cells. That there was appropriate cellular collagen IV staining indicates that the localization of cholera toxin was not due to lack of access of the molecule to binding sites in the basal and lateral domains. Similar results were obtained with an antibody against GM_1 (not shown).

Effect of Lipid Composition on $^{35}SO_4/SO_4$ Exchange

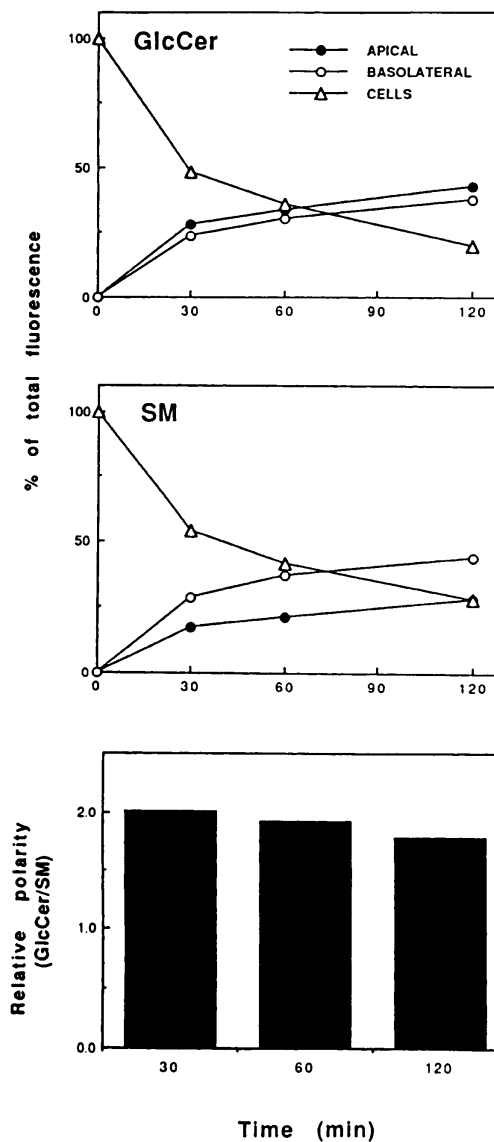Band 3 proteoliposomes composed of PC, SM, or SM +

Figure 1. Delivery of NBD-lipids in intercalated cells. The top panel shows the polarized delivery of Glc/Cer, the middle panel shows the polarized transport of SM, and the lower panel shows the relative polarity (Glc/Cer to SM ratio). The data shown are an average of six studies in two independent experiments. Shown are the results in cells that were seeded at low density, and identical results were obtained in cells seeded at high density, which were also performed in six studies.

30% GM_1 transported $^{35}SO_4$ in a time-dependent manner. This uptake was larger than that in the simultaneously determined protein-free liposomes or in proteoliposomes prepared with protein pretreated with the irreversible inhibitor of band 3, DIDS (Fig. 3). When plotted as the fractional uptake against time, the uptake exhibited first order kinetics; the rate coefficients were PC, −0.41 ± 0.02; SM, −0.31 ± 0.03; and SM + 30% GM_1, −0.48 ± 0.02 ($n = 6$, for each lipid). The addition of 30% GM_1 to SM increased the rate coefficient significantly ($P < 0.01$), and the PC values were intermediate between the two but not different from either. Proteoliposomes also differed in the isotope equilibrium level of $^{35}SO_4$, even though the total

Low Density
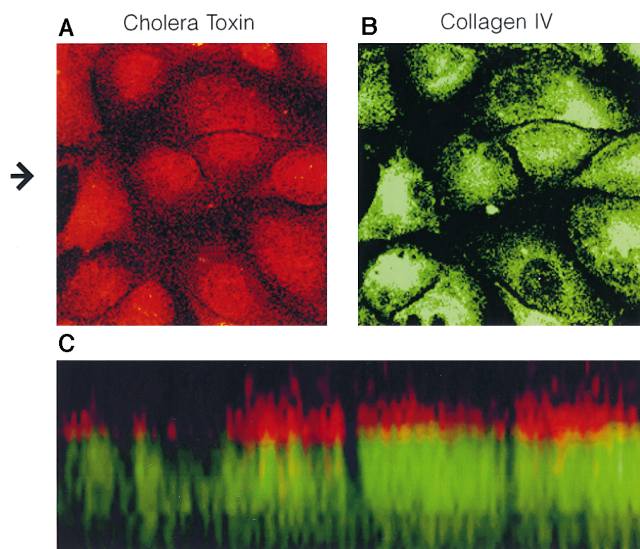
Figure 2. Confocal microscopic images showing apical expression of GM$_1$ using rhodamine-labeled cholera toxin B-subunit compared with cellular and basal expression of collagen IV in low-density intercalated cells. 20 z-sections of the sample were scanned using 488 nm (*green*) laser light and subsequently with 568 nm (*red*) light to avoid cross-talk between the two channels. *A* is the xy-projection of the brightly stained three apical sections (i.e., sections 9–11) of the red channel images (cholera toxin), and *B* is the xy-projection of three basolateral sections (i.e., 13–15) of green channel (collagen) images. The xz-section (*C*) at the indicated position was obtained from the combined RGB images. Labeled cholera toxin and antibodies to collagen IV were present in both apical and basolateral media. Identical results were obtained in cells seeded at high density. These are representative images of four independent experiments for each density of seeding.

amount of lipid and input protein used was the same. These kinetic parameters depend on the size of liposomes of different lipid composition, on the fraction that contained functional band 3, on the presence of multilamellar vesicles, and on the size distribution of liposomes in a given lipid mixture. Because of these concerns, it would not be possible to give a quantitative estimate of the effect of lipid composition on the turnover number of band 3. However, an order of magnitude type of information can be arrived at by using the measured uptake rate coefficients and the estimated amount of red cell ghost protein that is band 3 and the efficiency of incorporation of band 3 into different liposomes (see Materials and Methods). The rates in nmol/min per mg of band 3 were 180 $\pm$ 73 for PC, 215 $\pm$ 61 for SM, and 738 $\pm$ 230 for SM + 30% GM$_1$. Although there are no published results for the rate of $^{35}SO_4/SO_4$ exchange of rabbit band 3, those of human band 3 vary between 2,700 nmol/min per mg band 3 as measured in native red cells (Schnell et al., 1977) to values as low as 6 nmol/min per mg when band 3 was solubilized in detergent and reconstituted in PC vesicles (Kohne et al., 1983).

One of the characteristics of band 3 is that $^{35}SO_4$ transport is stimulated by the *trans* anion. Band 3 proteoliposomes were loaded with $^{35}SO_4$, and the extravesicular isotope was removed by passage through an anion exchange

resin. The liposomes were then diluted into media containing gluconate as the major anion or sulfate. Fig. 4 shows that in SM and SM + 30% GM$_1$ liposomes, there was a rapid efflux of $^{35}SO_4$ when the external anion was sulfate. In contrast, there was hardly any efflux in gluconate media.

Band 3 is a titrable carrier, hence $^{35}SO_4$ transport is pH sensitive (Gunn, 1979; Milanick and Gunn, 1982). Examination of the effect of symmetrical changes in pH on the initial rate of $^{35}SO_4/SO_4$ exchange (at 37°C) showed that PC liposomes exhibited the well-known stimulation of transport by acid pH (Fig. 5). In SM vesicles, the peak stimulation was shifted to pH 6. The mechanism by which bulk lipids exert their effect on the titrability of the carrier is unknown, but perhaps it involves changing the local environment of the titrable group such as might occur when the packing of the peptide chains is altered.

Effect of Lipid Composition on Sensitivity to DNDS

The effect of the reversible inhibitor, DNDS (Cabantchick and Greger, 1992), on $^{35}SO_4/SO_4$ exchange was studied by sonicating the proteoliposomes in the presence of the drug to generate equal concentrations of the drug inside and outside the proteoliposomes. Band 3 is nearly randomly incorporated into these liposomes. DNDS had no effect on $^{35}SO_4/SO_4$ exchange in protein-free liposomes, except at the 50 μM concentration where there was a slight decrease. In each study, we measured the 1-min uptake in band 3 proteoliposomes and the corresponding protein-free liposome in the presence and absence of different concentration of DNDS. There was a dose-dependent inhibition of the uptake (Fig. 6), and the apparent K_i (estimated from a Dixon plot) was 2 $\pm$ 1 μM in PC liposomes, while in SM liposomes it was 7 $\pm$ 3 μM (Fig. 6 *B*). The $K_{i,DNDS}$ of human band 3 for $^{35}SO_4/SO_4$ exchange was 2 μM (Schnell et al., 1977), and that for mouse band 3 in asolectin vesicle was 8 μM (Sekler et al., 1995).

When increasing amounts of GM$_1$ were added to SM liposomes, a larger portion of the flux became resistant to the effect of DNDS (Fig. 7). At 30% GM$_1$ (the ratio found in apical membranes [Kawai et al., 1974]) the inhibition at high concentrations of DNDS was only 30%. Other experiments where 5% GM$_1$ was used showed effects weaker than the 10% studies shown, while addition of 15% (*n* = 2) showed results intermediate between the 10 and 30% values. To reduce clutter, the latter two studies are not shown in Fig. 7. The GM$_1$ containing liposomes exhibited bona fide band 3–mediated transport; when they were made with DIDS-treated band 3, their $^{35}SO_4$ influx was lower than with the native protein (Fig. 3). When loaded with $^{35}SO_4$, their efflux rates were greater in the presence of external sulfate than that in external gluconate (Fig. 4).

Because the above studies were performed at pH 5.5 and at low ionic strengths, we repeated some of them at pH 7.5 and using 100 mM of added Na gluconate. The disulfonic stilbene DIDS at 200 μM completely inhibited the $^{35}SO_4/SO_4$ exchange in SM vesicles. But addition of GM$_1$ produced a resistance to inhibition: at 13% GM$_1$, $^{35}SO_4/SO_4$ exchange was 74% of that in the absence of 200 μM DIDS and at 26% GM$_1$, it was 97% of the uninhibited flux.

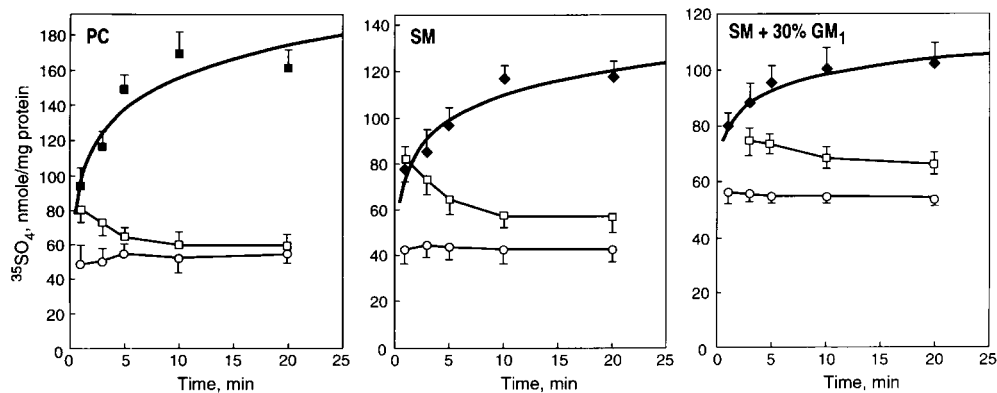Addition of 30% gangliosides to SM vesicles produced a highly nonlinear behavior on Dixon plots (Fig. 7, *dia-*

Figure 3. $^{35}SO_4$ uptake into phosphatidyl choline (*filled squares*), sphingomyelin (*filled diamonds*) or sphingomyelin + 30 GM_1 liposomes (*filled diamonds*), in the presence (*filled symbols*) or absence (*open circles*) of red cell ghost protein during the reconstitution. In some studies (*open squares*), red cell ghost protein was pretreated with 1 mM DIDS before reconstitution. These represent the averages of six independent studies for each lipid. In each of these studies, there was a simultaneously performed "control," which was either the protein-free liposomes ($n = 3$) or the DIDS-treated protein ($n = 3$). Every time point in each independent study is the average of triplicate measurements. Bars are the SEM. The results were fitted using a first order kinetics equation with the rate coefficients described in the text.

monds in right panel). Addition of 30% GM_1 to PC liposomes (Fig 7, *open squares*) also resulted in nonlinear inhibition kinetics, although the effect was less pronounced than with SM. When the sphingolipid moiety of GM_1, ceramide, was added to SM (also at 30%), the effect on the linearity of the Dixon plot was qualitatively similar to the addition of GM_1, but of a much smaller magnitude (Fig. 7, *filled circles*). These studies also suggest that both the carbohydrate and the sphingolipid portions of the ganglioside exert an effect on the characteristics of binding of DNDS to band 3, although the sugars seem to produce the greater effect.

One interpretation of these nonlinear plots is that the curve is composed of two portions: one is similar to the effect of DNDS on transport in the phospholipid liposomes without GM_1 (Fig. 6 *B*), and the other is a component totally insensitive to DNDS. The effect of GM_1 would then be to increase the DNDS-insensitive fraction. To examine this formally, a kinetic model was constructed (see Appendix). The assumptions were (*a*) that GM_1 molecules form homogeneous "rafts" because they interact with each other

but not with SM and (*b*) that when band 3 partitions into either phase, it has the same kinetic constants except for its sensitivity to DNDS. The experimental results of DNDS on sulfate exchange in liposomes composed of SM and SM + different concentrations of GM_1 (0, 5, 10, 15, and 30%) were then used to calculate, by nonlinear least squares, the best fit to Eq. A6 in the Appendix. From this fit, two parameters were calculated; the K_i was found to be 1.44 ± 0.29 µM, and the partition coefficient for band 3, γ, was found to be 2.79 ± 0.72. Although the K_i was lower than that calculated in pure SM vesicles in the data shown in Fig. 6 (7 ± 3 µM), the difference was not statistically significant. The best-fit curves are drawn in Fig. 7, and the results suggest that this model can describe these data with reasonable accuracy. The most interesting result of this kinetic analysis is the value of the partition coefficient, γ,
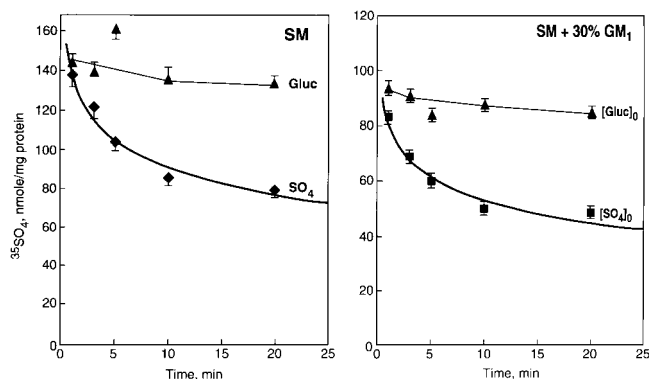

Figure 4. $^{35}SO_4$ efflux into media containing either gluconate (*triangles*) or sulfate (*diamonds or squares*) as the major anion. Band 3 was reconstituted into sphingomyelin (*diamonds*) or sphingomyelin + 30% GM_1 (*squares*). The results are the averages of three independent studies where each point was performed in triplicate. Bars are SEM.
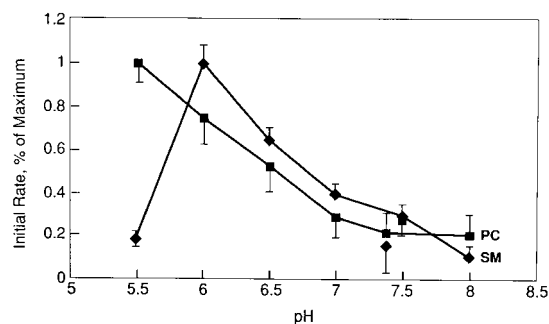

Figure 5. pH dependence of the initial rate (1-min uptake) of $^{35}SO_4/SO_4$ exchange in band 3 proteoliposomes. Comparison of PC (*squares*) and SM (*diamonds*). Results are averages of five independent experiments where each point was measured in triplicate. Liposomes had identical pH inside and out and the studies were conducted at 37°C. Results were normalized to the point with the highest rates. (Average net uptakes of the peak fluxes were PC, 2075 cpm; SM 966 cpm.) There was no effect of pH on the background uptake (PC, 830 cpm; SM, 386 cpm). Hence, we averaged all these fluxes and used that value to subtract them from the total uptake at each pH to obtain the plotted net uptakes. The shape of the curves was the same whether one used the total uptake or the net uptake.
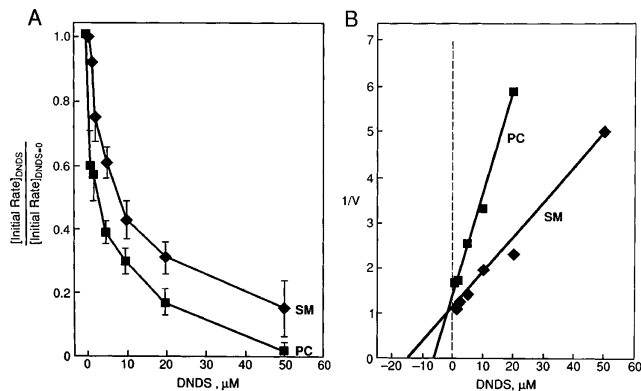
Figure 6. Inhibition of the initial rate of band 3–mediated $^{35}SO_4$/ SO_4 exchange by DNDS. DNDS was present at the same concentration inside and outside the vesicles. (*Left*) Inhibition was normalized to $^{35}SO_4$/SO_4 exchange measured in the absence of DNDS in the appropriate liposomes. All measurements were performed at pH 5.5 and at 37°C. Average of three independent experiments for each. The average flux in the absence of DNDS for PC vesicles was 145 nmol/min per mg protein and for SM vesicles it was 59 nmol/min per mg protein. (*Right*) Dixon plot of the results. The x-intercept of a Dixon plot is equal to the $K_i (1 + K_m/V_{max})$. Given that the concentration of SO_4 used is near the K_m, the actual K_i is close to one half of the intercept.

which implies that band 3 prefers to be in the GM_1 phase rather than the SM phase.

Discussion

Lipid composition of apical or basolateral membrane fractions are different, as demonstrated by studies in purified membrane fractions and more recently by kinetic analysis of delivery of fluorescent lipid precursors (Kawai et al., 1974; Simons and van Meer, 1988; van't Hof and van Meer, 1994). GSLs are preferentially delivered to the apical membranes in a variety of cells where they are enriched in the exofacial leaflet of the bilayer and exhibit very low rates of transbilayer movement (flip-flop). It was recently shown that in epithelial cells expressing multidrug resistance proteins, short chain Glc/Cer and phospholipid analogues can translocate across the apical plasma membrane lipid bilayer (van Helvoort et al., 1996). However, it is at present unclear whether this MDR-mediated mechanism also applies to endogenous GSLs whose rates of transbilayer movement is very low. It has been proposed that GSLs form rafts that do not mix well with other lipids in the Golgi (Simons and van Meer, 1988; Simons and Wandinger-Ness, 1990). If some membrane proteins have a selective affinity for these GSLs, then they could partition into these rafts and be carried to the apical membrane. One impetus for our studies was that apical anion exchange was insensitive to stilbenes, while basolateral exchange was readily inhibited (Schuster, 1985). That band 3 reconstituted in SM or PC liposomes was sensitive to DNDS is compatible with its in situ sensitivity to these inhibitors. GSLs and gangliosides were enriched in the apical membranes of the clonal cell line and the in vitro evidence of their ability to reduce the sensitivity of the anion exchanger to DNDS provides a potential explanation for why the apical AE1 in the β intercalated cell in vivo is so
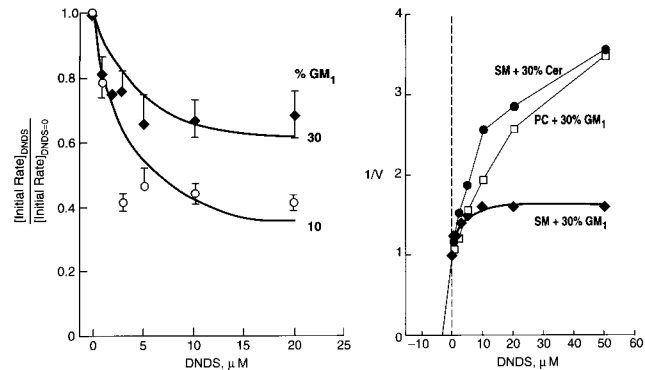
Figure 7. (*Left*) Inhibition of $^{35}SO_4$/SO_4 exchange via band 3 by DNDS in SM liposomes with different concentrations of GM_1. Results are averages of three independent experiments, 10% and 30% GM_1 with bars representing SEM. Using the 20 μM concentration, the 10% GM_1 was significantly different from the 0 and 30% GM_1 studies ($P < 0.05$ or better among the three). The lines are drawn using the model of the Appendix, with a γ of 2.79 and a K_i of 1.44 μM. Studies using 15 or 5% GM_1 were also used in the curve fitting procedure and showed equally good fit with the theoretical, but the data were not included to reduce the complexity of this figure. (*Right*) Inhibition of $^{35}SO_4$/SO_4 exchange via band 3 by DNDS in SM liposomes with 30% GM_1 (*diamonds*), SM liposomes with 30% ceramide (*circles*), and PC liposomes with 30% GM_1 (*squares*). The line for the SM + 30% GM_1 was drawn from the kinetic model of the Appendix, while for the other two conditions, it was drawn by eye. For each lipid, three independent experiments were performed and the averages shown. Each point was measured in triplicate.

resistant to the effect of disulfonic stilbenes. Others have reconstituted band 3 into various combinations of phospholipids, finding that addition of SM completely inhibited the rate of "specific" (i.e., DNDS-sensitive) $^{35}SO_4$/SO_4 exchange (Kohne et al., 1983), but these studies were done at 25°C, a temperature known to influence the state of SM, whose transition temperature is near 37°C (Barenholz et al., 1976). We are not aware of any published study of the effect of glycolipids on the inhibitory potency of disulfonic stilbenes.

In the pure phospholipid vesicles, the interaction between carrier and inhibitor seemed straightforward, giving a linear Dixon plot compatible with the known fact that DNDS is a competitive inhibitor of band 3. Addition of increasing amounts of GM_1 resulted in progressively nonlinear behavior (Fig. 7). One possible explanation of this complex behavior in GM_1 liposomes is that band 3 exists in two forms, one sensitive to DNDS and the other completely insensitive and that increasing the ganglioside concentration increases the fraction of band 3 that is insensitive, ultimately causing all of the protein to be insensitive. Kinetic analysis was undertaken to examine whether such a mechanism is plausible; indeed, the model fit the results reasonably well (Appendix and Fig. 7). This model started from the assumptions that GM_1 forms phases, such as the rafts discussed above, and that the kinetic properties of band 3 in the two phases are similar, with the exception of the inhibitory constants for DNDS. The results of the model are quantitatively compatible with the idea that when band 3 is in the GM_1 phase, it is insensitive to DNDS. Is there a plausible biochemical mechanism for this? It has

been demonstrated that when band 3 aggregates into tetramers or higher order oligomers in detergent micelles, its sensitivity to stilbenes is reduced (Schopfer and Salhany, 1992). Gangliosides might force aggregation of band 3, perhaps in these rafts. A surprising finding of the kinetic analysis was the value of the partition coefficient, γ, for band 3 between GM_1 and SM phases, which was 2.79, indicating that for any given amount of band 3, its concentration in GM_1 rafts will be three times higher than in SM. This makes the proposal of band 3 aggregation even more plausible.

The disulfonic stilbene DIDS binds covalently to a lysine in the transmembrane domain of band 3 (Cabantchik and Rothstein, 1974; Kaplan et al., 1976; Jennings et al., 1985; Wood et al., 1992). Recent mutagenesis experiments have identified two lysines that are critical for DIDS sensitivity, K558 and K869 (in the mouse sequence) (Wood et al., 1992). When these residues are mutated to methionine or asparagine, the DIDS sensitivity in the expressed single mutants is reduced by a factor of almost 10. When both are mutated, the affinity is reduced by a factor of almost 100. These lysines are located in the 5th and 13th putative transmembrane spanning regions (Kopito, 1990). Given that the length of DIDS is ~16 Å, these two loops must be close to each other in the three-dimensional structure of the protein in the lipid bilayer (Passow, 1986; Jennings, 1989; Kopito, 1990). It is interesting that GSLs and SM are present almost exclusively in the exofacial leaflet of the bilayer. These are the two lipids with the greatest effect on DIDS binding, a drug whose binding sites are themselves likely to be located in the external half of the loops (Jennings et al., 1985; Kaplan et al., 1976). As discussed above, it is conceivable that the high amount of GSLs or SM in the exofacial leaflets of the lipid bilayer might change the partition of band 3 between a conformation that is open to DIDS binding and one that is "closed." It is likely that the large size of DIDS makes it more sensitive to small changes in the dimensions of its binding pocket induced by the glycosphingolipids. Such postulated small changes might then not affect the binding of the transported anions, as seen in the minor differences in the kinetics of uptake in the different liposomes. Furthermore, the presence of hydroxy and amine residues in the sphingosine backbone enables sphingolipids to associate with each other or with other membrane components, such as gangliosides by hydrogen bonding, which can be strong enough to form microdomains (Thompson and Tillack, 1985). Because both SM and gangliosides are present in the exofacial leaflet, their sphingosine backbone might interact with the membrane spanning domains of band 3, reducing the exposure of the DIDS sensitive lysines.

Some epithelial membrane proteins are unpolarized while others, such as band 3, Na,K, ATPase, or the LDL receptor can be present in apical or basolateral membranes in different cells. When the Na,K ATPase is present in the apical membrane of one clone of MDCK, its sensitivity to ouabain was reduced (Hammerton et al., 1991). The bradykinin B2 receptor is located on the apical and basolateral membranes of tracheal epithelia. Its K_d for bradykinin is almost ten times lower when it is in the apical membrane and addition of GTP-γ-S has no effect on apical receptors but reduces the affinity of the basolateral receptor (Den-

ning and Welsh, 1991). Apical- and basolateral-type lipids might also be the cause of these differences. If so, this would form a new mechanism that can confer greater diversity in epithelial function. Our results also raise a note of caution regarding interpretation of structure from functional data obtained in different cell types. A number of transport proteins have been extensively characterized with respect to the kinetics of activation by substrates or inhibition by drugs. With the advent of molecular cloning of gene families, it is necessary to ascertain that the information obtained by heterologous expression is not confounded by cell type–specific problems such as different lipid composition of cell membranes. Indeed, Sekler et al. (1995) found that AE2, which was presumed to be much less sensitive to DIDS than AE1, turned out to have the same affinity when reconstituted into the same lipids.

Appendix

Kinetic Analysis of the Rate of Transport through the Band 3 Anion Exchanger

Our first assumption is that proteoliposomes are composed only of molecules of sphingomyelin, GM_1, and band 3. The number of molecules of each is given by the symbols SM, GM, and B, respectively. Furthermore, we assume that GM_1 forms a microdomain phase (i.e., "rafts") and that band 3 partitions between the two phases SM and GM. Each molecule of GM and SM has approximately the same surface area. Then, we can define a partition coefficient, γ, given

$$\gamma = \frac{\dfrac{B_{GM}}{GM}}{\dfrac{B_{SM}}{SM}} \tag{A1}$$

and

$$B_{TOTAL} = B_{GM} + B_{SM}. \tag{A2}$$

If B_{GM} is not inhibited by DNDS but B_{SM} is sensitive, then the transport rate v will be given by

$$v = k\left[\frac{B_{TOTAL} - B_{SM}}{1 + \dfrac{K}{[S]}} + \frac{B_{SM}}{1 + \dfrac{K}{[S]}\left(1 + \dfrac{[I]}{[K_i]}\right)}\right] \tag{A3}$$

where k is the maximum turnover number of band 3, [S] is the SO_4 concentration (26 mM), and K is the K_m for SO_4 (~30 mM; Gunn, 1979). [I] is the DNDS concentration and K_i is the inhibitory constant for DNDS. Rearranging and introducing Eqs. A1 and A2

$$v = kB_{TOTAL}\left[1 - \frac{1 - \dfrac{SM}{\gamma GM + SM}}{1 + \dfrac{K}{[S]}} + \frac{\dfrac{SM}{\gamma GM + SM}}{1 + \dfrac{K}{[S]}\left(1 + \dfrac{[I]}{K_i}\right)}\right] \tag{A4}$$

and

$$v_{I=0} = kB_{TOTAL}\left(\frac{1}{1 + \dfrac{K}{[S]}}\right) \tag{A5}$$

hence

$$\frac{v}{v_{[I]=0}} = 1 - \left[\frac{1}{1 + \gamma\left(\frac{GM}{SM}\right)}\right]\left[\frac{1}{\left(1 + \frac{K_i}{[I]}\right)\left(1 + \frac{[S]}{K}\right)}\right]. \qquad (A6)$$

References

Al-Awqati, Q. 1996. Plasticity in epithelial polarity of renal intercalated cells: targeting of the H⁺-ATPase and band 3. *Am. J. Physiol.* 270:C1571–C1580.

Barenholz, Y., J. Suurkuusk, D. Mountcastle, T.E. Thompson, and R.L. Biltoner. 1976. A calorimetric study of aqueous dispersions of natural and synthetic sphingomyelins. *Biochemistry.* 15:2441–2447.

Brosius, F.C., III, S.L. Alper, A.M. Garcia, and H.F. Lodish. 1989. The major kidney band 3 gene transcript predicts an amino terminal truncated band 3 polypeptide. *J. Biol. Chem.* 264:7784–7787.

Brown, D., S. Hirsch, and S. Gluck. 1988. An H⁺ ATPase in opposite plasma membrane domains in kidney epithelial cell subpopulations. *Nature.* 331: 622–624.

Cabantchik, Z.I., and A. Rothstein. 1974. Membrane proteins related to anion permeability. I. Localization of disulfonic stilbene binding sites involved in permeation. *J. Membr. Biol.* 15:207–226.

Cabantchik, Z.I., and R. Greger. 1992. Chemical probes for anion transporters of mammalian cell membranes. *Am. J. Physiol.* 31:C803–C827.

Casey, J.R., D.M. Lieberman, and R.A.F. Reithmeier. 1989. Purification and characterization of band 3 protein. *Methods Enzymol.* 173:494–512.

Cuatrecasas, P. 1973. Gangliosides and membrane receptors for cholera toxin. *Biochemistry.* 12: 3558–3566.

Denning, G.M., and M.J. Welsh. 1991. Polarized distribution of bradykinin receptors on airway epithelial cells independent of coupling to second messenger pathways. *J. Biol. Chem.* 266:12932–12938.

Drenckhahn, D., M. Olemann, P. Schaef, and V. Bennett. 1985. Colocalization of band 3 with ankyrin and spectrin at the basal membrane of intercalated cells of rat kidney. *Science.* 230:1287–1289.

Edwards, J.C., J. van Adelsberg, M. Rater, D. Herzlinger, J. Lebowitz, and Q. Al-Awqati. 1992. Conditional immortalization of bicarbonate-secreting intercalated cells from rabbit. *Am. J. Physiol.* 263:C521–C529.

Gottardi, C.J., L.A. Dunbar, M.J. Caplan. 1995. Biotinylation and assessment of membrane polarity: caveats and methodological concerns. *Am. J. Physiol.* 268:F285–295.

Gundersen, D., J. Orlowski, and E. Rodriguez-Boulan. 1993. Apical polarity of Na,K ATPase in retinal pigment epithelium is dependent on contact of neural retina. *J. Cell Biol.* 121:335–344.

Gunn, R.B. 1979. Transport of anions across red cell membranes. *In* Transport Across Single Biological Membranes. D.C. Tosteson, editor. Volume 2 in Membrane Transport in Biology. G. Giebisch, D.C. Tosteson and H.H. Ussing, editors. Springer Verlag. New York. 2:59–80.

Hammerton, R.W., K.A. Krezeminski, R.W. Mays, T.A. Ryan, D.A.Wollner, and W.J. Nelson. 1991. Mechanism for regulating cell surface distribution of Na,K Atpase in polarized epithelial cells. *Science.* 254:847–850.

Jennings, M.L. 1989. Structure and function of the red blood cell anion transport protein. *Annu. Rev. Biophys. Biophys. Chem.* 18:397–430.

Jennings, M.L., R. Monaghan, S.M. Douglas, and J.S. Niknish. 1985. Functions of extracellular lysine residues in human erythrocyte anion transport. *J. Gen. Physiol.* 86:653–669.

Kaplan, J.H., K. Skorah, and H. Passow. 1976. Sidedness of the inhibitory action of disulfonic acids on chloride equilibrium exchange and net transport across the human erythrocyte membrane. *FEBS Lett.* 62:182–185.

Kawai, K., M. Fujita, and N. Nakao. 1974. Lipid components of two different regions of an intestinal epithelial cell membrane of mouse. *Biochim. Biophys. Acta.* 369:222–233.

Kohn, O.H., P.F. Mitchell, and P.R. Steinmetz. 1990. Characteristics of apical Cl/HCO₃ exchanger of bicarbonate-secreting cells in turtle bladder. *Am. J. Physiol.* 258:F9–F14.

Kohne, W., B. Deuticke, and C.W. Haest. 1983. Phospholipid dependence of the anion transport system of the human erythrocyte membrane. Studies on reconstituted band 3/lipid vesicles. *Biochim. Biophys. Acta.* 730:139–150.

Kopito, R.R. 1990. Molecular biology of the anion exchanger gene family. *Int. Rev. Cytol.* 123:177–199.

Kudrycki, K.E., and G.E. Shull. 1989. Primary structure of the rat kidney band 3 anion exchange protein deduced from a cDNA. *J. Biol. Chem.* 264:8185–8192.

Landry, D.W., M. Reitman, E.J. Cragoe, Jr, and Q. Al-Awqati. 1987. Epithelial chloride channel: development of inhibitory ligands. *J. Gen. Physiol.* 90:779–798.

Lencer, W.I., C. Delp, M.R. Neutra, and J.L. Madara. 1992. Mechanism of cholera toxin action in a polarized human intestinal epithelial cell: role of vesicular traffic. *J. Cell Biol.* 117:1197–1209.

Lipsky, N.G., and R.E. Pagano. 1985. Intracellular translocation of fluorescent sphingolipids in cultured fibroblasts: endogenously synthesized sphingomyelin and glucocerebroside analogues pass through the Golgi apparatus en route to the plasma membrane. *J. Cell Biol.* 100:27–34.

Lisanti, M.P., and E. Rodriguez-Boulan. 1990. Glycophospholipid membrane anchoring provides clues to the mechanism of protein sorting in polarized epithelial cells. *Trends Biochem. Sci.* 15:113–118.

Milanick, M.A., and R.B. Gunn. 1982. Proton-sulfate cotransport: mechanism of H⁺ and sulfate addition to the chloride transporter of human red blood cells. *J. Gen. Physiol.* 79:87–113.

Pagano, R.E., and O.C. Martin. 1988. A series of fluorescent *N*-acylsphingosines: synthesis, physical properties, and studies in cultured cells. *Biochemistry.* 27:4439–4445.

Passow, H. 1986. Molecular aspects of band 3 protein mediated anion transport across the red blood cell membrane. *Rev. Physiol. Pharmacol. Biochem.* 103: 61–203.

Pathak, R.K., M. Yokodoe, R.E. Hammer, S.L. Hoffman, M.S. Brown, J.L. Goldstein, and R.W.G. Anderson. 1990. Tissue-specific sorting of the human LDL receptor in polarized epithelia of transgenic mice. *J. Cell Biol.* 112:863–872.

Schnell, K.F., S. Gerhardt, and A. Schoppe-Fredenburg. 1977. Kinetic characteristics of the sulfate self-exchange in human red blood cells and red blood cell ghosts. *J. Membr. Biol.* 28:319–350.

Schopfer, L.M., and J.M. Salhany. 1992. Factors determining the conformation and quaternary structure of isolated human erythrocyte band 3 in detergent solutions. *Biochemistry.* 31:12610–12617.

Schuster, V.L. 1985. Cyclic-AMP stimulated anion transport in rabbit cortical collecting duct: kinetics, stoichiometry and conductive pathways. *J. Clin. Invest.* 78:1621–1630.

Schuster, V.L. 1993. Function and regulation of collecting duct intercalated cells. *Annu. Rev. Physiol.* 55:267–288.

Schwartz, J.G., J. Barasch, and Q. Al-Awqati. 1985. Plasticity of functional epithelial polarity. *Nature.* 318:368–371.

Sekler, I., R.S. Lo, T. Mastrocola, and R.R. Kopito. 1995. Sulfate transport mediated by the mammalian anion exchangers in reconstituted proteoliposomes. *J. Biol. Chem.* 270:11251–11256.

Simons, K., and G. van Meer. 1988. Lipid sorting in epithelial cells. *Biochemistry.* 27:6197–6202.

Simons, K., and A. Wandinger-Ness. 1990. Polarized sorting in epithelia. *Cell.* 62:207–210.

Spiegel, S., G.R. Matyas, L. Cheng, and B. Sacktor. 1988. Asymmetric distribution of gangliosides in rat renal brush-border and basolateral membranes. *Biochim. Biophys. Acta.* 938:270–278.

Takito, J., C. Hikita, and Q. Al-Awqati. 1996. Hensin, a new collecting duct protein involved in the in vitro plasticity of intercalated cell polarity. *J. Clin. Invest.* 98:2324–2331.

Thompson, T.E., and T.W. Tillack. 1985. Organization of glycosphingolipids in bilayers and plasma membranes of mammalian cells. *Annu. Rev. Biophys. Chem.* 14:361–386.

van Adelsberg, J.S., J.C. Edwards, and Q. Al-Awqati. 1993. The apical Cl/HCO₃ exchanger of intercalated cells. *J. Biol. Chem.* 268:11283–11289.

van Adelsberg, J.S., J.C. Edwards, J. Takito, B. Kiss, and Q. Al-Awqati. 1994. An induced extracellular matrix protein reverses the polarity of band 3 in intercalated epithelial cells. *Cell.* 76:1053–1061.

van Helvoort, A., A.J. Smith, H. Sprong, I. Fritsche, A.H. van Schinkel, P. Borst, and G. van Meer. 1996. MDR-1, P-glycoprotein is a lipid translocase of broad specificity, while MDR3, P-glycoprotein specifically translocates phosphatidyl choline. *Cell.* 87:507–517.

van Meer, G., E.H.K. Stelzer, R.W. Wijnaendts-van-Resandt, and K. Simons. 1987. Sorting of sphingolipids in epithelial (Madin-Darby canine kidney) cells. *J. Cell Biol.* 105:1623–1635.

van't Hof, W., and G. van Meer. 1990. Generation of lipid polarity in intestinal epithelial (Caco-2) cells: sphingolipid synthesis in the Golgi complex and sorting before vesicular traffic to the plasma membrane. *J. Cell Biol.* 111: 977–986.

van't Hof, W., and G. van Meer. 1994. Lipid polarity and sorting in epithelial cells. *In* Cell Lipids: From Synthesis to Cell Biology. D. Hoekstra, editor. Academic Press, Orlando, FL. 539–563.

Wood, P.G., H. Muller, M. Sovak, and H. Passow. 1992. Role of Lys 558 and Lys 869 in substrate and inhibitor binding to the murine band 3 protein: a study of the effects of site-directed mutagenesis of the band 3 protein expressed in the oocytes of *Xenopus laevis. J. Membr. Biol.* 127:139–148.

Zurzolo, C., M.P. Lisanti, L. Nitsch, and E. Rodriguez-Boulan. 1993. Glycophosphatidylinositol-anchored proteins are preferentially targeted to the basolateral surface in Fischer rat thyroid epithelial cells. *J. Cell Biol.* 121:1031–1039.